SANDIA REPORT

SAND2004-4321
Unlimited Release
Printed September 2004

Relationships Among Certain Joint Constitutive Models

Daniel J. Segalman and Michael J. Starr, Sandia

Prepared by
Sandia National Laboratories
Albuquerque, New Mexico 87185 and Livermore, California 94550

Sandia is a multiprogram laboratory operated by Sandia Corporation,
a Lockheed Martin Company, for the United States Department of Energy's
National Nuclear Security Administration under Contract DE-AC04-94-AL85000.

Approved for public release; further dissemination unlimited.

Sandia National Laboratories

Issued by Sandia National Laboratories, operated for the United States Department of Energy by Sandia Corporation.

NOTICE: This report was prepared as an account of work sponsored by an agency of the United States Government. Neither the United States Government, nor any agency thereof, nor any of their employees, nor any of their contractors, subcontractors, or their employees, make any warranty, express or implied, or assume any legal liability or responsibility for the accuracy, completeness, or usefulness of any information, apparatus, product, or process disclosed, or represent that its use would not infringe privately owned rights. Reference herein to any specific commercial product, process, or service by trade name, trademark, manufacturer, or otherwise, does not necessarily constitute or imply its endorsement, recommendation, or favoring by the United States Government, any agency thereof, or any of their contractors or subcontractors. The views and opinions expressed herein do not necessarily state or reflect those of the United States Government, any agency thereof, or any of their contractors.

Printed in the United States of America. This report has been reproduced directly from the best available copy.

Available to DOE and DOE contractors from
U.S. Department of Energy
Office of Scientific and Technical Information
P.O. Box 62
Oak Ridge, TN 37831

Telephone: (865) 576-8401
Facsimile: (865) 576-5728
E-Mail: reports@adonis.osti.gov
Online ordering: http://www.doe.gov/bridge

Available to the public from
U.S. Department of Commerce
National Technical Information Service
5285 Port Royal Rd
Springfield, VA 22161

Telephone: (800) 553-6847
Facsimile: (703) 605-6900
E-Mail: orders@ntis.fedworld.gov
Online ordering: http://www.ntis.gov/ordering.htm

SAND2004-4321
Unlimited Release
Printed September 2004

Relationships Among Certain Joint Constitutive Models

Daniel J. Segalman and Michael J. Starr
Structural Dynamics Research Department
Sandia National Laboratories
P.O. Box 5800
Albuquerque, NM 87185-0847
djsegal@sandia.gov

Abstract

In a recent paper, Starr and Segalman demonstrated that any Masing model can be represented as a parallel-series Iwan model. A preponderance of the constitutive models that have been suggested for simulating mechanical joints are Masing models, and the purpose of this discussion is to demonstrate how the Iwan representation of those models can yield insight into their character. In particular, this approach can facilitate a critical comparison among numerous plausible constitutive models. It is explicitly shown that three-parameter models such as Smallwood's (Ramberg-Osgood) calculate parameters in such a manner that macro-slip is not an independent parameter, yet the model admits macro-slip. The introduction of a fourth parameter is therefore required. It is shown that when a macro-slip force is specified for the Smallwood model the result is a special case of the Segalman four-parameter model. Both of these models admit a slope discontinuity at the inception of macro-slip. A five-parameter model that has the beneficial features of Segalman's four-parameter model is proposed. This model manifests a force-displacement curve having a continuous first derivative.

Acknowledgment

Thanks to Todd Simmermacher, Dave Smallwood, and Tom Paez, whose conversations with us over the years have contributed significantly to this work.

Contents

Introduction . . . 7
The Smallwood Model . . . 8
  Masing Models . . . 8
  Features of the Smallwood/Ramberg-Osgood Model . . . 11
Parallel-Series Iwan Systems . . . 11
  Iwan Model Definition Form . . . 11
  All Masing Models are Also Iwan Models . . . 14
  System Identification from Displacement-Based Data . . . 14
  System Identification from Force-Based Data . . . 15
Inversion of the Ramberg-Osgood Model via Parallel-Series Iwan Systems . . . 15
Approximate Inversions . . . 16
  Doubly-Asymptotic Approximation . . . 16
  Singly-Asymptotic Approximation . . . 17
  Smallwood's Postulated Inverse . . . 21
Continuous and Discontinuous Force Displacement Slopes . . . 22
Conclusion . . . 23
References . . . 24
Appendix: Properties of the 5-Parameter Model . . . 25

Figures

1 *Schematic of a hysteresis loop which obeys Masing's hypothesis. The unloading and reloading curves are derived directly from the initial monotonic loading curve.* . . . 9
2 *Schematic of the parallel-series Iwan model.* . . . 12
3 *The density $\rho(\phi)$ for Jenkins elements corresponding to a Ramberg-Osgood model having $r = 1.5$. Such a model might be appropriate to simulate a mechanical joint.* . . . 17
4 *The force of the three-parameter model reaches a maximum and then declines. Only the portion of the curve to the left of the maximum can be used sensibly.* . . . 19
5 *The log-log plot of energy dissipation versus force shows the dissipation rate becoming infinite as the force amplitude approaches the max value available to it.* . . . 20
6 *The backbone and dissipation curves for the 5-parameter model for the case $F_S = 1$, $K_T = 1$, $\beta = 1$, $\chi = -1/2$, and $\lambda = -1/2$. Note that the slope of the backbone curve goes to zero as the displacement approaches macro-slip. The dissipation curve manifests a power-law dissipation at small load amplitudes.* . . . 26

This Page Intentionally Left Blank

Relationships Among Certain Joint Constitutive Models

Introduction

It would be well to give the historical basis and impetus for this work. The story begins in 2000 when Jeffrey Dohner [1] explored the construction of constitutive models for joints employing a close approximation to the Masing hypothesis [7] and using cubic and quartic polynomial representations for the backbone curve. Shortly afterward, David Smallwood et al.[2] constructed a symmetric hysteresis (Masing) model in which the backbone curve shared the response characteristics of the Ramberg-Osgood model [12]. It was recognized that energy dissipation in jointed structures was often approximately power-law in nature, at least at loads substantially lower than the force necessary to initiate macro-slip, so the Ramberg-Osgood model was a natural construction for use in the low-force regime.

Early in 2001, Dan Segalman [3] proposed an Iwan model that also predicted power-law behavior, though only in the region of small loads. In 2002, he proposed a similar 4-parameter constitutive model [4] that explicitly contained an independent parameter identifying the macro-slip force. Being Iwan representations, the Segalman models are also Masing models [5]. Although the use of distribution functions within the Iwan model may seem to be an additional step toward the construction of hysteretic response, it is shown below that those distribution functions afford clarifying insight and rigorous supporting mathematics for comparison and evaluation of competing constitutive models.

The most prominent properties of a joint when measured in one-dimensional experiments are:

- stiffness K_T manifest under small amplitude load
- the force F_S necessary to initiate macro-slip
- dissipation $D(F_0)$ per cycle as a function of load amplitude F_0 in harmonic experiments. For many joints and over large ranges of load, the dissipation is approximated reasonably well by a power-law relationship

  $$D(F_0) = C_0 F_0^{\alpha} \tag{1}$$

  though this is far from universally true.

The role of these properties in the various constitutive models listed above is presently described.

The Smallwood Model

Smallwood et al. [2] observed that a Ramberg-Osgood plasticity model coupled with an assumption of Masing behavior could predict a power-law dissipation over *all* force amplitudes.

The Ramberg-Osgood [12] plasticity model asserts that on initial monotonic loading, the applied force f and the resulting displacement u are related as

$$u = \left(\frac{F_R}{K_R}\right)\left(\frac{f}{F_R}\right)\left[1 + \left(\frac{f}{F_R}\right)^{r-1}\right] \tag{2}$$

where the exponent r is greater than 1.0 and the normalizing force F_R roughly separates the region of near-linear behavior ($f < F_R$) from the softening region ($f > F_R$). Examination of Eq. (2) will show that K_R actually is the low-force stiffness (represented in the following as K_T).

Smallwood et al. [2] accommodated macro-slip by asserting that the applied force saturates at a nominal yield level.

Masing Models

As a means of modeling the Bauschinger effect [6], Masing [7] considered a collection of ten parallel elasto-plastic material elements, each with identical elastic modulus but with a different yield stress level. At the time, it was believed that the discrete yield levels were phenomenologically linked with different orientations of grains within the material, although it is now generally accepted that the Bauschinger effect arises from local variations in dislocation density and the development of back stress along active slip planes due to dislocation pile-ups. During load reversal each of Masing's discrete elements exhibits plasticity only after going through twice its initial elastic range. The intrinsic behavior of this model is thus: hysteretic paths obtained during cyclic loading are of the same form as the monotonic loading, except for an expansion by a factor of two (shown in Figure 1).

Masing was the first to assert the above relationship between the initial loading curve and the hysteresis loop, which is now commonly referred to as Masing's hypothesis.

The monotonic loading curve is often referred to as the *backbone* curve. The backbone curve can be used to present displacement in terms of force

$$u = G(f) \tag{3}$$

or to present the force in terms of displacement

$$f = F(u) \tag{4}$$

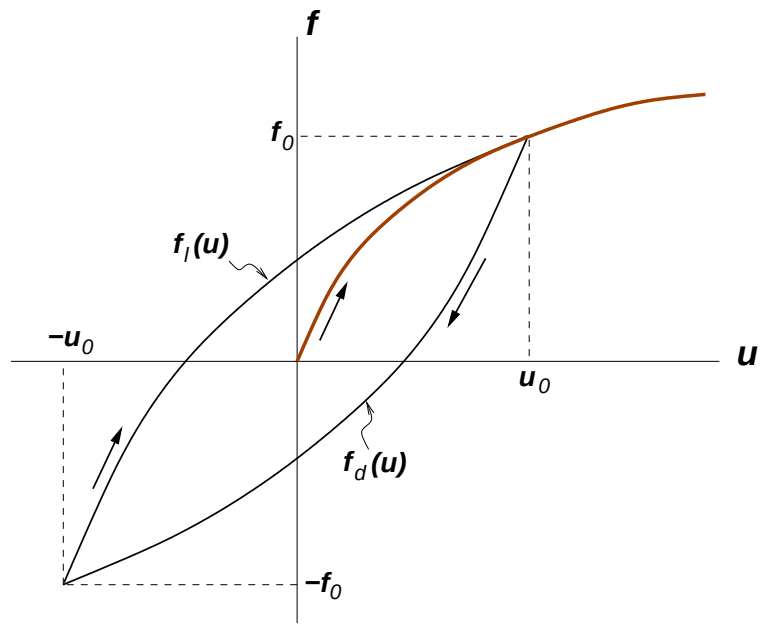

Figure 1. *Schematic of a hysteresis loop which obeys Masing's hypothesis. The unloading and reloading curves are derived directly from the initial monotonic loading curve.*

The mathematical representation of Masing's hypothesis can be phrased as

$$u_d(f) = u_0 - 2G\left(\frac{f_0 - f}{2}\right) \tag{5}$$

which states that the unloading displacement, u_d, as a function of applied force, is given by the displacement at load reversal, u_0 minus twice the function, G of Eq. (3). The reloading displacement, u_l, is the negative of the unloading displacement with a negative argument

$$u_l(f) = -u_d(-f) = -u_0 + 2G\left(\frac{f_0 + f}{2}\right) \tag{6}$$

Note that Eqs. (5) and (6) can each be inverted to provide corresponding displacement based relationships:

$$f_d(u) = f_0 - 2F\left(\frac{u_0 - u}{2}\right) \tag{7}$$

and

$$f_l(u) = -f_0 + 2F\left(\frac{u_0 + u}{2}\right) \tag{8}$$

Examination of Eqs. (5) and (6) or Eqs. (7) and (8) will show that the lower curve of the hysteresis loop is obtained by reflecting the upper curve both vertically and horizontally. When a hysteresis loop exhibits this particular symmetry, it satisfies the Masing relationship.

Further, the energy dissipation per cycle under harmonic loading can be expressed in terms of the backbone curve:

$$D(f_0) = -8\int_0^{f_0} G(f)\,\mathrm{d}f + 4f_0u_0 \tag{9}$$

and

$$D(u_0) = 8\int_0^{u_0} F(u)\,\mathrm{d}u - 4u_0f_0 \tag{10}$$

Substitution of Eq. (2) into Eq. (9) obtains the energy dissipation per cycle for the Ramberg-Osgood model:

$$D_{\mathrm{R-O}} = 4\left(\frac{r-1}{r+1}\right)(F_R^2/K_R)\,(f_0/F_R)^{1+r} \tag{11}$$

which is indeed the power-law relation that Smallwood et al. [2] desired. We note that the Ramberg-Osgood exponent r is related to the power-law dissipation slope by $r = \text{slope} - 1$. To provide power-law slopes of the desired range ($2 \leq \text{slope} \leq 3$), the exponent must satisfy $1 \leq r \leq 2$.

The original Masing hypothesis is valid only for cases of steady-state cyclic behavior or loading between fixed limits. However, Masing's hypothesis has been extended by following two simple rules (Jayakumar [8]) so that arbitrary hysteretic response can be obtained. The first rule states that the equation of any hysteretic response curve is obtained by applying the Masing hypothesis using the latest point of loading reversal. The second rule asserts that if an active curve crosses a curve described in a previous cycle, the current curve follows that of the previous cycle. In this manner, the response to any load history can be computed from the backbone curve and a record of all load reversals. It is this generalized Masing rule that is employed by Smallwood et al. [2]

Features of the Smallwood/Ramberg-Osgood Model

Though the Ramberg-Osgood model discussed above could be a reasonable model for one-dimensional joint behavior, there are some serious limitations. The first is that most of our finite element codes are displacement based - they expect constitutive models to return a force increment resulting from a given displacement increment. It would be valuable to invert this model.

Other serious limitations of this model concern the Masing assumption. The experimental data show that the symmetries inherent to the Masing assumption are not supported empirically. On the other hand such subtleties may be beyond the reach of simple constitutive models and the economy of expression and efficiency of computation facilitated by the Masing hypothesis may be adequate return for that loss of fidelity.

To make good use of the Ramberg-Osgood model, it is necessary to be able to both invert it and compare it in a commensurate manner with other alternative constitutive models. Iwan's parallel-series systems provide that capability.

Parallel-Series Iwan Systems

Iwan Model Definition Form

The parallel-series model is the more frequently treated of the two major Iwan [9] models. Figure 2 shows a collection of N parallel spring-slider or Jenkins elements that constitute a parallel-series Iwan system. Each Jenkins element consists of a linear spring with stiffness k_i in series with a Coulomb damper with break-free force $\tilde{\phi}_i$. The Jenkins elements are indexed in order of their slider strengths.

For an imposed displacement, u, the total force acting through the system is given by

$$f = \sum_{\tilde{\phi}_i \leq k_i\, u} \tilde{\phi}_i + \sum_{\tilde{\phi}_i \geq k_i\, u} k_i u \tag{12}$$

where the first summation includes all those Jenkins elements which have slipped and the second summation includes all those elements which remain elastic. Like Iwan, it is assumed that all the springs have the same stiffness, k, and the number of elements having a break-free strength $\tilde{\phi}$ is expressed in terms of a density, $\tilde{\rho}(\tilde{\phi})$. The density, sometimes referred to as a distribution function, is a non-negative function whose domain is all possible values of $\tilde{\phi}$ (all positive numbers). Typically it is assumed that

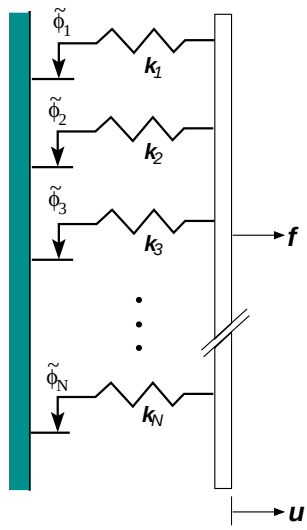

Figure 2. *Schematic of the parallel-series Iwan model.*

each spring has a stiffness, k, so the resultant force in the system is

$$f = \int_0^{ku} \tilde{\phi}\tilde{\rho}(\tilde{\phi})\mathrm{d}\tilde{\phi} + ku\int_{ku}^{\infty} \tilde{\rho}(\tilde{\phi})\mathrm{d}\tilde{\phi} \tag{13}$$

It is then convenient to remove the stiffness, k, from the above equation by using the following changes of variable due to Segalman [4]:

$$\begin{aligned} \phi &= \tilde{\phi}/k \\ \rho(\phi) &= k^2\tilde{\rho}(k\phi) \end{aligned}$$

Eq. (13) now becomes

$$f = \int_0^{u} \phi\rho(\phi)\mathrm{d}\phi + u\int_{u}^{\infty} \rho(\phi)\mathrm{d}\phi \tag{14}$$

If the system is moved to a certain state of displacement, u_0, undergoes a reverse displacement to $-u_0$ and is then re-displaced to u_0, a hysteresis loop with Masing type symmetry will result. The force-displacement relationship at any given state during reverse displacement involves three elemental contributions, namely, those that have 1) yielded during initial displacement and yielded during reversal, 2) yielded

during initial displacement and are still elastic during reversal, and 3) those that were elastic during initial displacement and remain elastic during reversal. The form of the relationship is

$$f_d(u) = -\int_0^{(u_0-u)/2} \phi\rho(\phi)\mathrm{d}\phi + \int_{(u_0-u)/2}^{u_0} (u - u_0 + \phi)\rho(\phi)\mathrm{d}\phi + u\int_{u_0}^{\infty} \rho(\phi)\mathrm{d}\phi \tag{15}$$

for the reverse motion. Similar calculations show that

$$f_l(u) = \int_0^{(u_0+u)/2} \phi\rho(\phi)\mathrm{d}\phi + \int_{(u_0+u)/2}^{u_0} (u + u_0 - \phi)\rho(\phi)\mathrm{d}\phi + u\int_{u_0}^{\infty} \rho(\phi)\mathrm{d}\phi \tag{16}$$

for motion back in the positive direction.

Eqs. (15) and (16) can be shown to satisfy Eqs. (7) and (8) respectively where F in those last equations is taken to be the left hand side of Eq. (14). This establishes that every parallel-series Iwan model is also a Masing model.

The force (stress) response to an arbitrary displacement history can be calculated from

$$f(t) = \int_0^{\infty} \rho(\phi)[u(t) - x(t,\phi)]\,\mathrm{d}\phi \tag{17}$$

and

$$\dot{x}(t,\phi) = \begin{cases} \dot{u} & \text{if } \|u - x(t,\phi)\| = \phi \text{ and } \dot{u}\,(u - x(t,\phi)) > 0 \\ 0 & \text{otherwise} \end{cases} \tag{18}$$

where the quantities $x(t,\phi)$ are states that capture the amount of slipping that takes place for each species (characterized by a value of ϕ) of Jenkins element. It is the presence of these quantities that enables parallel-series Iwan elements to accommodate arbitrary load/displacement histories. Note that it is guaranteed that $\|u - x(t,\phi)\| \leq \phi$.

From examination of Eqs. (17) and (18), the tangent stiffness at low force levels is

$$K_T = \int_0^{\infty} \rho(\phi)\,\mathrm{d}\phi \tag{19}$$

and the yield force is

$$F_S = \int_0^{\infty} \phi\rho(\phi)\,\mathrm{d}\phi \tag{20}$$

In modeling joints, F_S is the force necessary to initiate macro-slip.

The energy dissipation of displacing the Iwan system a distance u_0 is four times the integral of the product of slider force (ϕ) and slider displacement ($u_0 - \phi$) times the density of such sliders ($\rho(\phi)$):

$$D_{\mathrm{I}}(u_0) = 4 \int_0^{u_0} \rho(\phi)\, \phi\, [u_0 - \phi]\, d\phi \tag{21}$$

(This equation can also be derived from Eq. (10)).

All Masing Models are Also Iwan Models

The authors have shown elsewhere [5] that all Masing models can be represented - in principle - as parallel-series Iwan models. The proof observes that any two Masing constitutive models that have identical backbone curves must be equivalent models. Further, given any backbone curve, an Iwan model can be constructed [10] that shares that backbone. Since Iwan models are also Masing models, that Masing model can also be represented by an Iwan model.

The qualifying words "in principle" are used because the identification of the parameters of the Iwan model corresponding to a given Masing model is sometimes a challenge.

System Identification from Displacement-Based Data

Iwan showed [10] how the density can be derived through the second derivative of Eq. (14)

$$\rho(\phi) = -\left.\frac{\mathrm{d}^2 f}{\mathrm{d}u^2}\right|_{u=\phi} \tag{22}$$

If the ordinate of the backbone curve is unbounded and the backbone increases asymptotically to a linear response $\lim_{u\to\infty} f(u)/u = K_\infty > 0$, the Iwan system determined above reproduces the original Masing model only up to that limiting stiffness:

$$f(t) = \int_0^\infty \rho(\phi)[u(t) - x(t,\phi)]\, \mathrm{d}\phi + K_\infty u \tag{23}$$

where the constant K_∞ is selected so that

$$K_T = \left.\frac{\mathrm{d}f}{\mathrm{d}u}\right|_{u=0} = \int_0^\infty \rho(\phi)\, \mathrm{d}\phi + K_\infty \tag{24}$$

The stiffness K_∞ corresponds to a Dirac delta function in ρ at $\phi = \infty$. Song et al. [11] discussed this additional stiffness extensively.

System Identification from Force-Based Data

For Masing models where displacement is given in terms of force, Eq. (22) cannot be applied directly. Given a Masing model that presents the backbone displacement u_R in terms of the applied force f_R:

$$u_R = G(f_R) \tag{25}$$

an inverse function F is sought such that it returns backbone force in terms of displacement:

$$f_R = F(u_R) \tag{26}$$

where F and G are inverse functions

$$G(F(u_R)) = u_R \tag{27}$$

In general, explicit inversion of G to obtain F is not possible, but the chain rule provides a means of deriving the relationship between derivatives

$$\left.\frac{\mathrm{d}F(u)}{\mathrm{d}u}\right|_{u=G(f_R)} = \frac{1}{(\mathrm{d}G/\mathrm{d}f_R)} \tag{28}$$

and

$$\left.\frac{\mathrm{d}^2F(u)}{\mathrm{d}u^2}\right|_{u=G(f_R)} = -\frac{\mathrm{d}^2G}{\mathrm{d}f_R^2}\Big/\left(\frac{\mathrm{d}G}{\mathrm{d}f_R}\right)^3 \tag{29}$$

Inversion of the Ramberg-Osgood Model via Parallel-Series Iwan Systems

Applying the operator of Eq. (29) to the Ramberg-Osgood model (Eq. (2)), obtains the Iwan distribution function corresponding to this model:

$$(F_R/K_R^2)\,\hat{\rho}(u(f)) = \frac{r(r-1)(f/F_R)^{r+1}}{((f/F_R) + r(f/F_R)^r)^3} \tag{30}$$

The above and Eq. (2) can be used to plot the Iwan distribution function versus displacement. This relationship is plotted in dimensionless form for the case $r = 1.5$ in Figure 3. The asymptotic behavior seen in this figure can be deduced by combining Eqs. (2) and (30) for both small and large values of f:

$$(F_R/K_R^2)\hat{\rho}(u) = \begin{cases} r(r-1)(uK_R/F_R)^{r-2} & \text{for small } u \quad (31) \\ ((r-1)/r^2)(uK_R/F_R)^{(1-2r)/r} & \text{for large } u \quad (32) \end{cases}$$

These asymptotic curves intersect at

$$u^* = (F_R/K_R)\, r^{3r/(1-r^2)} \tag{33}$$

The above leads to the definition of dimensionless slider strength

$$\phi = u\, K_R/F_R \tag{34}$$

and a dimensionless distribution function

$$\rho(\phi) = (F_R/K_R^2)\, \hat{\rho}(\phi F_R/K_R) \tag{35}$$

Note that the asymptotic representation for small arguments (Eq. (31)) has the integrable singularity ϕ^χ (where $\chi = \text{slope} - 3$) that Segalman [3] demonstrated to be necessary to obtain power-law behavior in the region of small loads.

Approximate Inversions

The density ρ can be represented arbitrarily well with the asymptotes (Eqs. (31) and (32)) for small and large values of the abscissa along with spline (or other) interpolation over the intermediate region. This representation and Eq. (17) provides a nearly exact inversion of the Ramberg-Osgood model. Of course more concise representations for ρ would be desirable as well.

Doubly-Asymptotic Approximation

The density ρ can be approximated by just the asymptotes of Eqs. (31) and (32). This is not a particularly bad approximation. To the author's knowledge, it has not yet been explored.

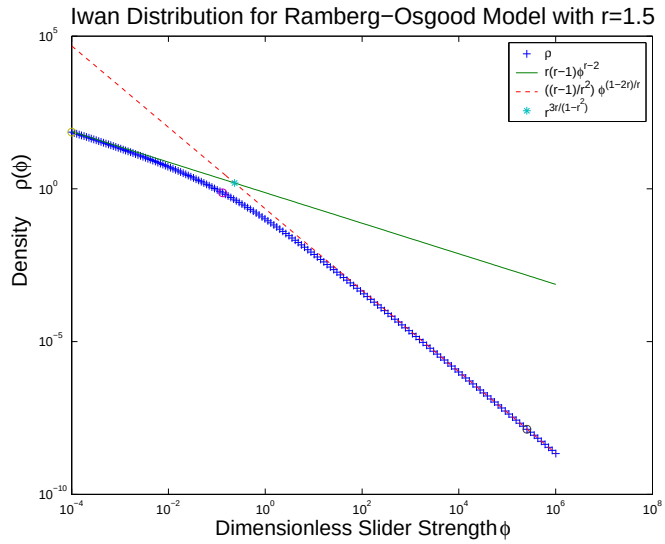

Figure 3. *The density $\rho(\phi)$ for Jenkins elements corresponding to a Ramberg-Osgood model having $r = 1.5$. Such a model might be appropriate to simulate a mechanical joint.*

Singly-Asymptotic Approximation

Segalman's Three-Parameter Iwan Model

Segalman [3] introduced a constitutive model in 2001 that could predict power-law behavior in the region of low forces. This consisted of the parallel-series Iwan model defined by

$$\rho(\phi) = \begin{cases} R\,\phi^{\chi} & \text{for } 0 < \phi < \phi_{\max} \\ 0 & \text{for } \phi > \phi_{\max} \end{cases} \tag{36}$$

in parallel with a stiffness

$$K_0 = K_T - \int_0^{\phi_{\max}} R\phi^{\chi} \mathrm{d}\phi \tag{37}$$

where $\phi_{\max}$ bounds the anticipated joint displacements. Parameters R and χ are selected to reproduce exactly the asymptote of Eq. (31). Because the approximation for the Jenkins population distribution is *exact* for $u < u^*$, the energy dissipation will also be exact for imposed cyclic deformations within that range.

Referring to Eq. (21), the energy dissipation per cycle under harmonic loading is

$$D_{\mathrm{S}_3}(u_0) = \frac{4Ru_0^{3+\chi}}{(\chi+2)(\chi+3)} \tag{38}$$

Since much of the glue holding this modeling approach together is the Masing hypothesis, it is worth exploring the backbone curve associated with this model.

$$f(u) = \int_0^u R\phi^\chi \phi d\phi + u \int_u^{\phi_{\max}} R\phi^\chi d\phi + u\, K_0 \tag{39}$$

$$= K_T u - \frac{R}{(\chi+1)(\chi+2)} u^{\chi+2} \tag{40}$$

In the above form, it is fairly clear that for oscillatory loading at small force amplitudes f_0, the resulting displacement amplitudes will be proportional to the force amplitude $u_0 \sim f_0$ and

$$D \sim {f_0}^{3+\chi} \tag{41}$$

as expected. On the other hand, behavior at large forces is far from obvious. Examination of Eq. (40) shows that the force resulting from monotonic displacement reaches a maximum at

$$\hat{u} = \left(\frac{K_T(\chi+1)(\chi+2)}{R} \right)^{\frac{1}{\chi+1}} \tag{42}$$

In order to make dimensionless plots, a reference force $\hat{F}$ introduced from which the following dimensionless quantities are defined

$$\begin{array}{rr} \tilde{f} = f/\hat{F} & \tilde{u} = K_T\, u/\hat{F} \\ \tilde{R} = R\hat{F}^{\chi+1}/K_T^{\chi+2} & \tilde{D} = DK_T/\hat{F} \end{array}$$

The dimensionless backbone curve is plotted in Figure 4 for the case of $\tilde{R} = 1$ and $\chi = -0.5$. Here the force does indeed reach a maximum. This maximum force can be associated with the inception of macro-slip.

A corresponding plot of dimensionless dissipation versus dimensionless force under oscillatory loading for the case of $\tilde{R} = 1$ and $\chi = -0.5$ is presented in Figure 5. Here the dissipation goes as force to the $3 + \chi$ power for small loads. On the other hand,

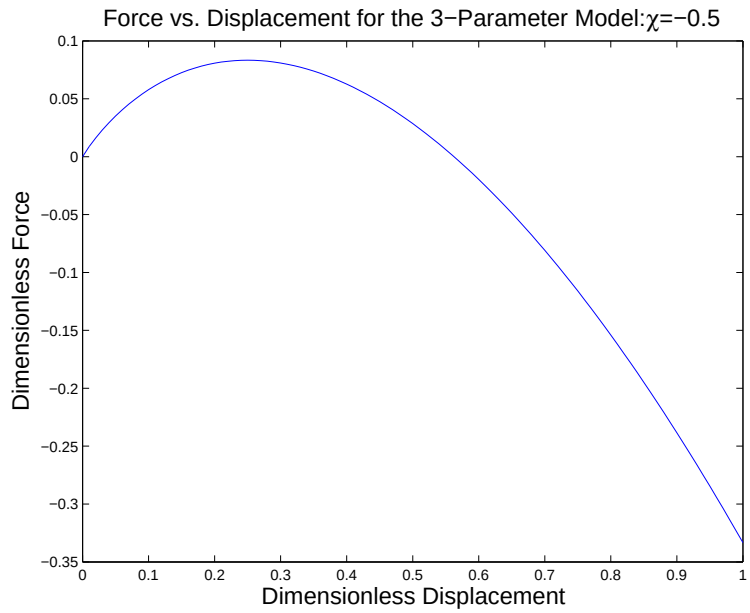

Figure 4. *The force of the three-parameter model reaches a maximum and then declines. Only the portion of the curve to the left of the maximum can be used sensibly.*

as the force approaches it maximum value, the rate of dissipation approaches infinity. This behavior is consistent with the initiation of macro-slip.

The disturbing element of this model is that the three parameters R, χ, and K_T are determined by stiffness and by dissipation at low force; they have nothing to do with macro-slip. The macro-slip force should be defined independently of the low-force stiffness and the dissipation.

Segalman's 4-Parameter Model

The 4-parameter Iwan model [4] was introduced both to accommodate a macro-slip force and to permit tuning of the dissipation rate at large force levels as well as small.

Here again, starting with the left asymptotic curve to the Iwan representation for the Ramberg-Osgood model (Eq. (31)) a displacement $u_{\max}$ at which macro-slip occurs is explicitly specified. Additionally, in order to accommodate macro-slip, the spring in parallel with the Iwan system is removed.

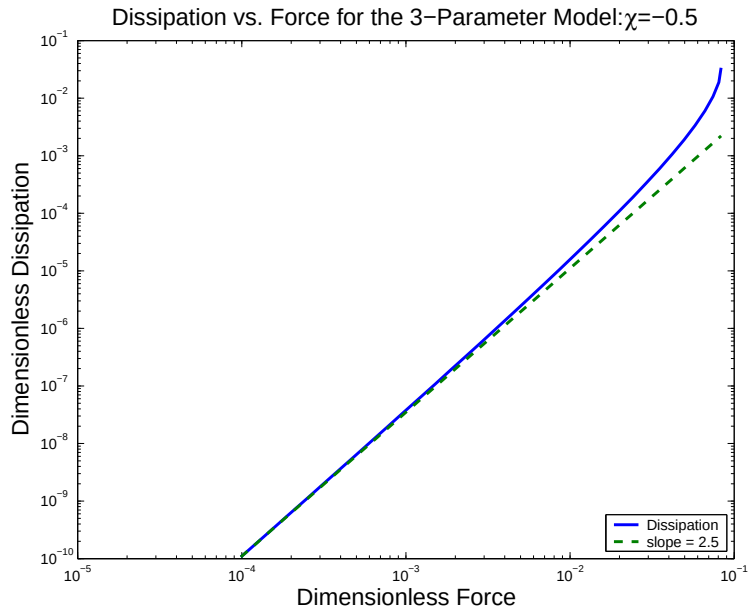

Figure 5. *The log-log plot of energy dissipation versus force shows the dissipation rate becoming infinite as the force amplitude approaches the max value available to it.*

A density is postulated

$$\rho(\phi) = R\,\phi^{\chi}\left[H(\phi) - H(\phi - u_{\max})\right] + S\delta(\phi - u_{\max}) \tag{43}$$

where H is the Heaviside function. Note the addition of the parameter S. Parameters R and χ are associated with the power-law distribution at low forces, $u_{\max}$ is associated with macro-slip, and S contributes to both stiffness and yield load.

Of the four parameters χ is dimensionless, $u_{\max}$ has dimension length, S has dimension force/length, and R has fractional dimension. This is a sub-optimal combination. Ideally, parameters of fractional dimension should be avoided and dimensionless parameters are preferred over those with dimension. Additionally parameters that most directly relate to measurable properties are preferred. With this in mind, a preferred set of parameters is $\{K_T, F_S, \chi, \beta\}$ where F_S is the force at micro-slip and β is defined by

$$S = \beta\left(\frac{R u_{\max}^{\chi+1}}{\chi+1}\right) \tag{44}$$

The remaining old parameters are expressed in terms of the new as follows:

$$u_{\max} = \left(\frac{F_S}{K_T}\right)\left(\frac{1+\beta}{\beta + (\chi+1)/(\chi+2)}\right) \tag{45}$$

and

$$R = \frac{F_S(\chi+1)}{u_{\max}^{\chi+1}\left(\beta + (\chi+1)/(\chi+2)\right)} \tag{46}$$

The dimensionless parameters χ and β are found so as to best fit the dissipation data from oscillatory load experiments. Per reference [4], the force amplitude F_0 during oscillatory loading is parameterized by a scalar $\psi : 0 \leq \psi \leq 1$

$$F_0 = F_S\,\psi\,\frac{(\beta+1) - \psi^{\chi+1}/(\chi+2)}{\beta + (\chi+1)/(\chi+2)} \tag{47}$$

as is the dissipation per cycle with respect to ψ

$$D = \psi^{\chi+3}\,4\left(\frac{F_S^2}{K_T}\right)\left(\frac{(\beta+1)(\chi+1)}{(\beta + \frac{\chi+1}{\chi+2})^2\,(\chi+2)(\chi+3)}\right) \tag{48}$$

Parameters χ and β are found via numerical optimization so that a plot of D from Eq. (48) against F_0 from Eq. (47) best reproduces the experimental dissipation data.

This model has been fit to several data sets successfully [4]. Of course given incomplete experimental data, the "best" model parameters are always found. If the tangent stiffness at very low loads is not available, it is extrapolated from stiffnesses measured at larger loads. If there is no macro-slip data from which to deduce F_S, normal loads in the joint could be estimated and multiplied by a coefficient of restitution.

Smallwood's Postulated Inverse

Smallwood et al. [2] postulated an inverse to the Ramberg-Osgood model which is identical to Segalman's three-parameter model, though none of the authors fully realized the connection at the time. Segalman presented his model in terms of the Iwan density whereas Smallwood et al. [2] presented their model in terms of a backbone curve (equivalent to Eq. (40)) and the Masing conditions.

Smallwood [15] sometimes introduces macro-slip by modifying his backbone curve to flatten out at some point (u_S, F_S) where $u_S < \hat{u}$ (see Eq. (42)). The mathematical form of the modified backbone is

$$f_{\text{DOS}}(u) = \left(K_T\, u \; - \; \frac{R}{(\chi+1)(\chi+2)} u^{\chi+2} \right) [1 - H(u - u_{_S})]$$

$$+ \left(K_T\, u_{_S} \; - \; \frac{R}{(\chi+1)(\chi+2)} u_{_S}^{\chi+2} \right) H(u - u_{_S}) \tag{49}$$

The corresponding Iwan distribution is

$$\rho_{\text{DOS}}(\phi) = R\phi^{\chi}\, [1 - H(u - u_{_S})] + \left(K_T - \frac{R}{(\chi+1)} u_{_S}^{\chi+1} \right) \delta(\phi - u_{_S}) \tag{50}$$

which is a special case of Segalman's four-parameter model.

Continuous and Discontinuous Force Displacement Slopes

The δ - function was placed at the termination of the support of the distribution function in Eq. (43) the stiffness K_T and macro-slip force F_S could be specified separately. The disadvantage of admitting the delta function is that it causes a discontinuity of slope in the backbone curve: the slope to the right of macro-slip is zero, while the slope just prior to macro slip is

$$\left. \frac{\mathrm{d}f}{\mathrm{d}u} \right|_{u=u_{\text{max}}^{-}} = \lim_{u \to u_{\text{max}}} \int_{u}^{u_{\text{max}}} \rho(\phi) \mathrm{d}\phi = S \tag{51}$$

This problem can be obviated by replacing the δ - function in Eq. (43) with some slightly less singular function that lives primarily on the right hand side of the interval $(0, u_{\text{max}})$. One candidate for that function is suggested by the distribution function that captures the Mindlin solution for the shearing of contacting spheres:

$$\rho_{_{\text{M}}}(\phi) = S\, (u_{\text{max}} - \phi)^{\lambda}\; [H(\phi) - H(\phi - u_{\text{max}})] \tag{52}$$

where $\lambda = -1/2$. To eliminate the discontinuous slope, a 5-parameter model can be chosen

$$\rho_5(\phi) = \left[R\, \phi^{\chi} + S\, (u_{\text{max}} - \phi)^{\lambda} \right] \; [H(\phi) - H(\phi - u_{\text{max}})] \tag{53}$$

where $-1 < \lambda \leq 1$. It is apparent that the tangent stiffness of the backbone curve is continuous all the way through macro-slip. The cost of this approach is that yet another parameter has been introduced to the constitutive model. Strategies for finding all five parameters from the (generally limited) experimental data can be devised or λ can be fixed at some nominal value such as $\lambda = -1/2$.

Properties of this model are outlined in the appendix.

Conclusion

The appeal of the Ramberg-Osgood model for a numerical simulation of joints is that it is simple and defined by parameters that can be related to elementary experimental parameters. The force-based nature of this model makes it ill-suited to displacement-based structural dynamics applications, so there is strong motivation to find displacement approximations that could be used instead.

Because all Masing models can be represented as Iwan models, this problem can be posed as that of finding tractable Iwan population distributions that approximate that of the Ramberg-Osgood model. Most efforts up to now capture the low-force asymptotic behavior of the Ramberg-Osgood model but differ on how they accommodate higher forces.

The displacement-based model of Smallwood et al. [2] and Segalman's three-parameter Iwan model are shown to be equivalent by observing that they have the same backbone curves and are both Masing models. These models manifest a yield load that cannot be set independently of the small force stiffness and dissipation.

Segalman's four-parameter Iwan model resolves this difficulty while retaining the appropriate asymptotic behavior at low-forces by specifying a compact support for the Iwan distribution function.

Limitations of all of the above formulations must be kept in mind. First, as discussed above, any Masing model will show the symmetries of Eqs. (5) through (8) which are generally not found experimentally. This visible divergence may not be a serious issue, but it should be remembered. Another consideration is that where a yield load is specified in the above models, the corresponding slope in the backbone curve is generally non-zero. In Eq. (43) this discontinuity in slope is due to the presence of the δ - function. This issue might be resolved by using a weaker singularity.

References

[1] Dohner, J. L., 2000, A reduced order, one dimensional model of joint response, Proceedings of the SAVIAC held November 7 - 8, 2000 in Washington, DC.

[2] Smallwood, D. O., Gregory, D. L., and Coleman, R. G., 2001, A three parameter constitutive model for a joint which exhibits a power law relationship between energy loss and relative displacement, Proceedings of the Shock and Vibration Symposium held November 12-16, 2001 in Destin, FL.

[3] Segalman, D. J., 2001, An Initial Overview of Iwan Modeling for Mechanical Joints, SAND2001-0811, Sandia National Laboratories, Albuquerque, NM.

[4] Segalman, D. J., 2002, A four-parameter Iwan model for lap-type joints, SAND2002-3828, Sandia National Laboratories, Albuquerque, NM.

[5] Starr, M. J. and Segalman, D. J., 2004, Functional Relations within Masing Models, submitted to the *International Journal of Plasticity*.

[6] Bauschinger, J., 1886, On the change of position of the elastic limit of iron and steel under cyclic variations of stress, *Mitt. Mech. Tech. Lab. Munchen*, **13**, pp. 1-115.

[7] Masing, G., 1926, Self-stretching and hardening for brass, *Proc.* 2nd *Int. Cong. Applied Mechanics*, pp. 332-335.

[8] Jayakumar, P., 1987, Modeling and identification in structural dynamics, Report No. EERL 87-01, California Institute of Technology, Pasadena.

[9] Iwan, W. D., 1966, A distributed-element model for hysteresis and its steady-state dynamic response, *Journal of Applied Mechanics*, **33**, pp. 893-900.

[10] Iwan, W. D., 1967, On a class of models for the yielding behavior of continuous and composite systems, *Journal of Applied Mechanics* **34**, pp. 612-617.

[11] Song, Y., Hartwigsen, C. J., McFarland, D. M., Vakakis, A. F., and Bergman, L. A., 2004, Simulation of dynamics of beam structures with bolted joints using adjusted Iwan beam elements, *Journal of Sound and Vibration*, **273**(1-2), pp. 249-276.

[12] Ramberg, W., Osgood, W. R., 1943, Description of stress-strain curve by three parameters, *NACA Technical Note No. 902*.

[13] Stephens, R. I., Fatemi, A., Stephens, R. R., Fuchs, H. O., 2000, Metal Fatigue in Engineering, 2nd Edition, Wiley, New York.

[14] Mostaghel, N., Byrd, R. A., 2002, Inversion of Ramberg-Osgood equation and description of hysteresis loops, *Int. J. Non-Linear Mech.*, **37**, pp. 1319-1335.

[15] Smallwood, D. O., 2004, private communication.

Appendix: Properties of the 5-Parameter Model

Of course a preferred set of parameters would lean heavily toward dimensionless parameters, parameters of integer dimension, and parameters that are directly measurable. One such set of preferred parameters would be $\{\chi, \lambda, \beta, F_S, K_T\}$, where

$$\beta = \left(\frac{S\, u_{\max}^{\lambda+1}}{1+\lambda}\right) / \left(\frac{R\, u_{\max}^{\chi+1}}{1+\chi}\right) \tag{A-1}$$

Solving for the old parameter set in terms of the new set:

$$u_{\max} = \left(\frac{F_S}{K_T}\right)\left(\frac{(\beta+1)\,(2+\lambda)\,(2+\chi)}{\beta\,(2+\chi)\;+\;(2+\lambda)\,(\chi+1)}\right) \tag{A-2}$$

$$R = K_T\,\frac{(\chi+1)}{u_{\max}^{\chi+1}\,(\beta+1)} \tag{A-3}$$

and

$$S = K_T\,\frac{\beta\;(\lambda+1)}{u_{\max}^{\lambda+1}\,(\beta+1)} \tag{A-4}$$

The backbone curve behaves as

$$f(s\,u_{\max}) = \frac{R\,u_{\max}^{2+\chi}\,s\;\left[(2+\chi)-s^{1+\chi}\right]}{(\chi+1)\,(2+\chi)} + \frac{S\,u_{\max}^{2+\lambda}\left[1-(1-s)^{2+\lambda}\right]}{(\lambda+1)\,(2+\lambda)} \tag{A-5}$$

The dissipation behaves as

$$D(s\,u_{\max}) = 4\,\frac{R\,s^{3+\chi}\,u_{\max}^{3+\chi}}{(3+\chi)\,(2+\chi)}$$

$$+\,4\,\frac{S\,u_{\max}^{3+\lambda}\left[-2+s\;(3+\lambda)+(1-s)^{\lambda}\left[2-(3-\lambda)\,s-2\,\lambda\,s^2+(\lambda+1)s^3\right]\right]}{(\lambda+1)\,(2+\lambda)\,(3+\lambda)} \tag{A-6}$$

The shapes of the backbone and dissipation curves for the case of $F_S = 1$, $K_T = 1$, $\beta = 1$, $\chi = -1/2$, and $\lambda = -1/2$ are shown in Figure A6. The slope of the backbone curve goes to zero as the displacement approaches macro-slip and the dissipation curve manifests a power-law dissipation at small load amplitudes. These two properties result from the asymptotic properties of ρ_5 at small and large values of its argument.

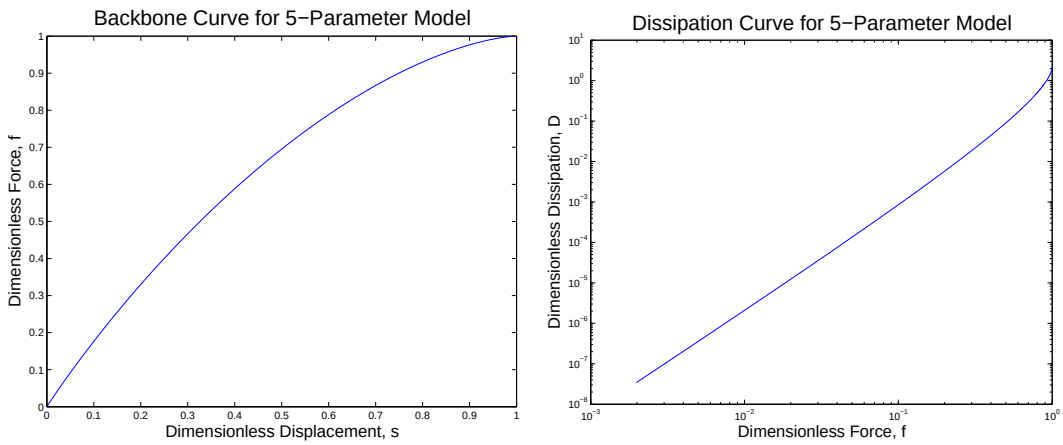

Figure 6. *The backbone and dissipation curves for the 5-parameter model for the case* $F_S = 1$, $K_T = 1$, $\beta = 1$, $\chi = -1/2$, *and* $\lambda = -1/2$. *Note that the slope of the backbone curve goes to zero as the displacement approaches macro-slip. The dissipation curve manifests a power-law dissipation at small load amplitudes.*

DISTRIBUTION:

1 Professor Ivo Babuska
Department of Aerospace Engineering
& Engineering Mechanics
University of Texas at Austin
105 W. Dean Keeton Street, SHC 328
Austin, TX, 78712

1 Dr. Edward Berger
Department of Mechanical, Industrial,
and Nuclear Engineering
P.O. Box 210072
Cincinnati, OH 45221-0072

5 Prof. Lawrence A. Bergman
University of Illinois
306 Talbot Lab
104 S. Wright St.
Urbana, IL 61801

1 Dr. Scott Doebling
Los Alamos National Laboratory, MS P946
Los Alamos, NM 87545

1 Dr. Jason Hinkle
Aerospace Engineering Sciences
Campus Box 429
University of Colorado
Boulder, CO 80309-0429

1 Prof. Raouf A. Ibrahim
College of Engineering
2119 Engineering Bldg.
Mechanical Engineering Department
Wayne State University
Detroit, MI 48202

1 Prof. Lee Peterson
Aerospace Engineering Sciences
Campus Box 429
University of Colorado
Boulder, CO 80309-0429

1 Dr. Chris Pettit
AFRL/VASD,
Bldg. 146, 2210 Eighth St.,
Wright Patterson AFB
OH 45433

1 Prof. D. Dane Quinn
Department of Mechanical Engineering
College of Engineering
The University of Akron
107b Auburn Science and Engineering Center
Akron, OH 44325-3903

1 Prof. Joseph C. Slater
Wright State University
Dept. of Mech. and Mat. Engg
209 Russ Center
3640 Colonel Glenn Highway
Dayton, OH 45435

1 Dr. Y.C. Yiu
Lockheed Martin Missiles & Space
Organization E4-20 Bldg 154
1111 Lockheed Martin Way
Sunnyvale, CA 94089

1 MS 380
Alvin, Kenneth F , 9142

1 MS 380
Bhardwaj, Manoj K , 9142

1 MS 380
Heinstein, Martin W , 9142

1 MS 380
Pierson, Kendall Hugh , 9142

1 MS 380
Reese, Garth M , 9142

1 MS 384
Morgan, Harold S. , 9140

1 MS 384
Peterson, Carl W. , 9100

1 MS 553
Smallwood, David O , 9124

1 MS 555
Gregory, Danny L , 9122

1 MS 555
Resor, Brian R , 9122

1 MS 557
Simmermacher, Todd W , 9124

1 MS 557
Baca, Thomas J , 9125

1 MS 557
Mayes, Randall L , 9125

1 MS 557
Paez, Thomas L , 9133

1 MS 824
Moya, Jaime L , 9130

1 MS 825
Hermina, Wahid , 9110

1 MS 828
Pilch, Martin , 9133

1 MS 834
Johannes, Justine E , 9114

1 MS 847
Wilson, Peter J. , 9120

1 MS 847
Bitsie, Fernando , 9124

1 MS 847
Redmond, James M , 9124

10 MS 847
Segalman, Daniel J , 9124

10 MS 847
Starr, Michael J. , 9124

1 MS 847
Wojtkiewicz, Steven F Jr , 9124

1 MS 847
Red-Horse, John R , 9133

1 MS 847
Urbina, Angel , 9133

1 MS 893
Pott, John , 9123

1 MS 1073
Dohner, Jeffrey L. , 1769

1 MS 1310
Sumali, Hartono , 9124

1 MS 9018
Central Technical Files, 8945-1

2 MS 0899
Technical Library, 9616